

# Optimum Surface Properties of Oxidized Implants for Reinforcement of Osseointegration: Surface Chemistry, Oxide Thickness, Porosity, Roughness, and Crystal Structure

Young-Taeg Sul, DDS, PhD<sup>1</sup>/Carina Johansson, PhD<sup>2</sup>/Ann Wennerberg, DDS, PhD<sup>3</sup>  
Lee-Ra Cho, DDS, PhD<sup>4</sup>/Beom-Seok Chang, DDS, PhD<sup>5</sup>/Tomas Albrektsson, MD, PhD<sup>6</sup>

**Purpose:** To investigate detailed surface characterization of oxidized implants in a newly invented electrolyte system and to determine optimal surface oxide properties to enhance the bone response in rabbits. **Materials and Methods:** A total of 100 screw-type titanium implants were prepared and divided into 1 control group (machine-turned implants) and 4 test groups (magnesium ion-incorporated oxidized implants). Forty implants were used for surface analyses. A total of 60 implants, 12 implants from each group, were placed in the tibiae of 10 New Zealand white rabbits and measured with a removal torque test after a healing period of 6 weeks. **Results:** For the test groups, the oxide thicknesses ranged from about 1,000 to 5,800 nm; for the control group, mean oxide thickness was about 17 nm. The surface morphology showed porous structures for test groups and nonporous barrier film for the control group. Pore diameter ranged from  $\leq 0.5 \mu\text{m}$  to  $\leq 3.0 \mu\text{m}$ . In regard to surface roughness, arithmetic average height deviation (Sa) values varied from 0.68 to 0.98  $\mu\text{m}$  for test implants and 0.55  $\mu\text{m}$  for control implants; developed surface ratio (Sdr) values ranged from 10.6% to 46% for the test groups and were about 10.6% for the control group. A mixture of anatase and rutile-type crystals were observed in the test groups; amorphous-type crystals were observed in the control group. After a healing period of 6 weeks, removal torque measurements in all 4 test groups demonstrated significantly greater implant integration as compared to machine-turned control implants ( $P \leq .033$ ). **Discussion:** Determinant oxide properties of oxidized implants are discussed in association with bone responses. Of all surface properties, RTVs were linearly increased as relative atomic concentrations of magnesium ion increase. **Conclusions:** Surface properties of the oxidized implants in the present study, especially surface chemistry, influenced bone responses. The surface chemistry of the optimal oxidized implant should be composed of approximately 9% magnesium at relative atomic concentration in titanium oxide matrix and have an oxide thickness of approximately 1,000 to 5,000 nm, a porosity of about 24%, and a surface roughness of about 0.8  $\mu\text{m}$  in Sa and 27% to 46% in Sdr; its oxide crystal structure should be a mixture of anatase- and rutile-phase crystals. INT J ORAL MAXILLOFAC IMPLANTS 2005;20:349–359

**Key words:** bone responses, implant surfaces, oxidized titanium implants, porosity, surface chemistry

<sup>1</sup>Assistant Professor, Department of Biomaterials/Handicap Research, Institute for Surgical Sciences, Göteborg University, Göteborg, Sweden.

<sup>2</sup>Professor, Department of Technology/Medical Technology, Örebro University, Örebro, Sweden.

<sup>3</sup>Professor, Departments of Biomaterials/Handicap Research and Prosthetic Dentistry/Dental Material Science, Göteborg University, Göteborg, Sweden.

<sup>4</sup>Associate Professor, Research Institute of Oral Science, Kangnung National University, Kangnung, Korea.

<sup>5</sup>Associate Professor, Department of Periodontics, Kangnung National University, Kangnung, Korea.

<sup>6</sup>Professor, Chairman, and Head, Department of Biomaterials/Handicap Research, Institute for Surgical Sciences, Göteborg University, Göteborg, Sweden.

**Correspondence to:** Dr Young-Taeg Sul, Department of Biomaterials/Handicap Research, Institute for Surgical Sciences, Göteborg University, Box 412, SE-405 30 Göteborg, Sweden. Fax: +46 31 773 2941. E-mail: young.taeg.sul@hkf.gu.se

Over the last 10 to 15 years, a number of investigations involving surface innovations of clinical implants have been carried out, particularly with regard to topographic changes. So-called “rouger” implants have been produced using etching, blasting, or hybrid techniques. However, the chemical composition of implant surfaces is mainly titanium oxide (TiO<sub>2</sub>). In fact, titanium metal normally inherits an air-formed surface oxide; a “native oxide layer” of a few nanometers is spontaneously formed during the manufacture of machine-turned implants. The excellent biocompatibility of titanium implants is related to the TiO<sub>2</sub> surface. Further modifications of the surface oxide properties of an implant have potential to ensure clinically favorable performance.

Several surface modification technologies have been introduced to control the surface oxide properties. Ion beam–based surface modification processes such as ion implantation, ion beam assisted/enhanced deposition, plasma source ion implantation (PSII), plasma immersion ion implantation (PIII), and plasma source immersion ion implantation (PSIII) have been used to modify implant surface chemistry and have demonstrated promising results in different biologic applications.<sup>1–4</sup> However, there are problems with these techniques for manufacturing screw-type implants because of the “line-of-sight limitations.” Thermal oxidization by heat treatment can cause brittleness and weak adhesion strength between the oxide layer and substrate over the critical temperature of some 500°C.<sup>5,6</sup> Sol-gel–processed implants have also shown promising in vivo results.<sup>7–9</sup> Electrochemically oxidized implants are currently being used clinically, and improved experimental and clinical performance has been reported.<sup>10,11</sup>

An international consensus agreement<sup>12</sup> was reached on the theoretical importance of surface properties for biologic response in 1985. However, there has been a paucity of investigation on the role and importance of surface oxide properties of titanium implants in in vivo studies, particularly in regard to surface chemistry.

A series of experiments using oxidized implants with various surface properties has been conducted by the authors and associates.<sup>13–21</sup> Implants processed by microarc oxidation (MAO) demonstrated significantly improved bone responses. Variations in surface chemistry and the subsequent influence on bone tissue reactions have been reported using implants that incorporated magnesium, calcium, sulfur, or phosphorus.<sup>18–21</sup> Based on previous results, 2 action mechanisms of osseointegration of oxidized implants have been proposed: (1) mechanical interlocking through bone growth in pores and (2) biochemical bonding.<sup>22</sup>

The purpose of the present study was to investigate optimal surface oxide properties of implants that were incorporated with magnesium ion for enhancement of bone response. The properties investigated included surface chemistry, oxide thickness, porosity, roughness, and crystal structure. The specific aim was to assess the role of the surface chemistry on the bone response. The hypothesis currently favored in regard to surface chemistry postulates biochemical bonding as an action mode for osseointegration, inducing faster and stronger integration of the implant in bone. Such biochemical bonding is believed to satisfy clinical demands for immediate/early loading and improved performance in compromised bone.

Oxidized implants were prepared using the MAO method.<sup>13,14</sup> To be able to validate what surface properties might be responsible for corresponding results, detailed surface characterizations were performed using various surface analytic techniques. In addition to the surface property analysis, removal torque was measured 6 weeks after placement of implants in the tibiae of rabbits.

## MATERIALS AND METHODS

### Implant Design and Preparation

A total of 100 screw-type commercially pure titanium implants, 3.0 mm in diameter and 7.2 mm in length, were manufactured. The implants were divided into 1 control group (machine-turned implants) and 4 test groups (magnesium ion–incorporated oxidized implants); each group comprised 12 implants. The test groups were designated Mg1, Mg2, Mg3, and Mg4; oxide thickness increased with group number. The electrochemical oxidation method employed in the present study has been described in previous studies.<sup>13,14</sup> In brief, all test implants were prepared using MAO methods at the galvanostatic mode. Two platinum plates with surface areas of 32 cm<sup>2</sup> were used as counter electrodes at both sides of the titanium anode. Currents and voltages were continuously recorded at intervals of 1 second by an IBM computer (IBM, Armonk, NY) interfaced with a direct-current power supply. Ripple was controlled to less than 0.1%.

### Surface Analysis

Forty implants were used for surface analyses: 2 implants per group for chemical analysis, 3 implants per group for morphology and pore characteristics, 1 implant per group for crystal structure, and 2 implants per group for surface roughness. Surface chemistry was analyzed by x-ray photoelectron spectroscopy (XPS; ESCALAB 250; Thermo Electron/VG Scientific, Waltham, MA). The XPS spectra were recorded using normal Al K $\alpha$  radiation (1486.8 eV) with a 200- $\mu$ m-wide probing beam. The outmost surfaces of the implants were etched with argon ions of an ion energy of 5 keV and a beam current of 0.3  $\mu$ A for 150 seconds, corresponding to 2 nm in thickness, resulting in removal of surface contaminants. The oxide thickness was measured with scanning electron microscopy (SEM, JSM-5800; JEOL, Tokyo, Japan) on cross sections of the test implants prepared by the metallurgical method of nickel plating. The oxide thickness of controls was evaluated by continuous sputter etching with 4 K eV argon ion in Auger electron spectroscopy (AES; model PHI 650; Physical Electronics, Chanhassen, Minnesota).

Overall surface morphology was characterized by SEM. Pore characteristics of test implants were determined with an image analysis system (Image Inside; Japan Focus Co, Tokyo, Japan). The crystal structure of the implant surface was determined by using low-angle x-ray diffraction with a thin film collimator (X'Pert PRO-MNR, Philips, Amsterdam, The Netherlands) on a plate-type sample prepared with the same electrochemical parameters as the test screw-type implants. The step size was 0.02 degrees between 15 and 70 degrees of measured scan. Spectra were recorded using Cu K $\alpha$  radiation (0.154056 Å) generated at an acceleration voltage of 35 kV and a current of 25 mA.

The surface roughness was measured with optical interferometry (MicroXamTM; ADE Phase Shift, Tucson, AZ). Two implants were selected and measured at 3 thread tops, 3 thread valleys, and 3 thread flanks each, for a total of 18 measurements per group.

### Animals and Surgical Technique

A total of 10 mature New Zealand white rabbits (mean weight 2.8 kg) were used in this study, which was approved by the animal ethics committee at Göteborg University. For surgery the animals were anesthetized with intramuscular injections of fentanyl-fluanisone (Hypnorm; Janssen, Saunderton, England) at a dose of 0.5 mL per kg body weight and intraperitoneal injections of diazepam (Valium; Roche, Basel, Switzerland) at a dose of 2.5 mg per animal. The skin and fascial layers were opened and closed separately. The periosteal layer was gently pulled away from the surgical area and was not resutured. During all surgical drilling sequences, low rotary drill speeds (not exceeding 2,000 rpm) and saline cooling were used. Three implants were placed in each tibia (6 implants per rabbit). The implants were placed in a predetermined randomized design to enable multiple comparisons.<sup>23</sup> The animals were kept in separate cages. The tibiae were allowed to bear weight immediately after surgery. After a follow-up period of 6 weeks, the animals were sacrificed by intravenous injections of pentobarbital (Pentobarbitalum, Apoteksbolaget, Uppsala, Sweden).

### Evaluations of the Bone Response

Bone response was evaluated using removal torque measurements. The removal torque instrument utilized a strain gauge transducer to test implant stability. It measured the peak loosening torque in Ncm. Thus, the torque removal measurement can be regarded as a 3-dimensional test roughly reflecting the interfacial shear strength between bone tissue and the implant.<sup>22,24</sup> The electronic device ensured a fixed rotation rate, in contrast to hand-controlled

devices, to eliminate operator error, and it has been shown to achieve high reproducibility and low operator sensitivity.<sup>22,24</sup> The present study employed a newly developed axis-alignment table to ensure that the rotation axis was kept in a straight line between the transducer and the implant. This alignment table was designed to correct a 3-dimensional adjustment on the micrometer scale.

### Statistics

Data are presented as means  $\pm$  SD. Removal torque values were analyzed using 2-way analysis of variance (ANOVA). Post hoc tests of removal torque values were performed using the Tukey method for multiple comparisons. Differences were considered statistically significant at  $P \leq .05$  and highly significant at  $P < .001$ .

## RESULTS

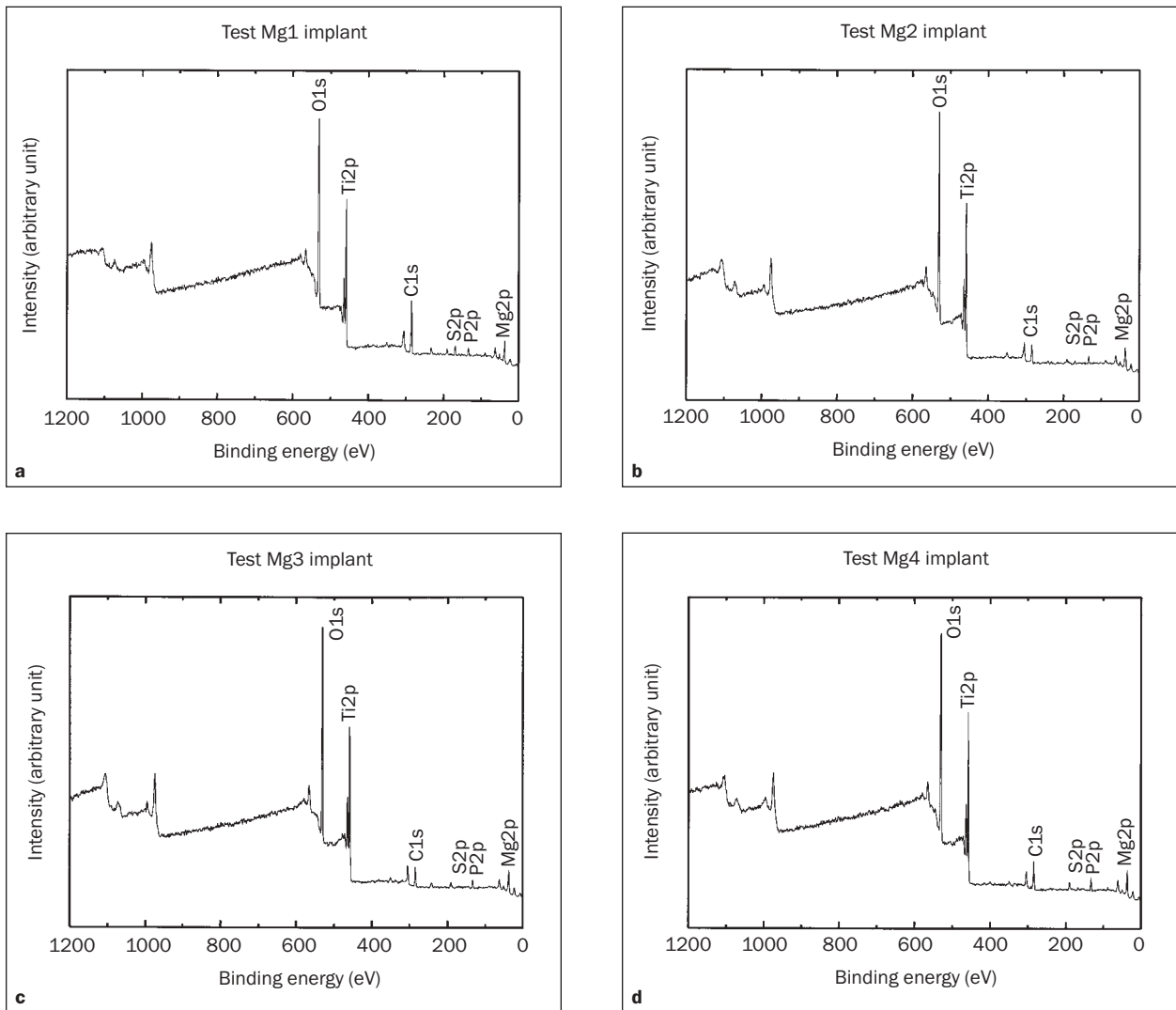
### Surface Characteristics

Figure 1 shows the XPS survey spectra of the test implants. High-resolution XPS spectra in Fig 2 revealed the binding energy of test Mg implants at Ti 2p, O 2p, Mg 2p, and C 1s. This indicated that the chemical composition of the surface oxide of test implants consisted mainly of magnesium incorporated into the TiO<sub>2</sub> matrix, ie, magnesium titanate and TiO<sub>2</sub>. The relative atomic concentrations of magnesium at the as-received surface of test implants were 8.36% for Mg1, 8.74% for Mg2, 8.97% for Mg3, and 9.33% for Mg4.

The mean oxide thicknesses were 1,060  $\pm$  140 nm (n = 15) for the Mg1 implants, 3,440  $\pm$  660 nm (n = 15) for the Mg2 implants, 5,190  $\pm$  500 nm (n = 15) for the Mg3 implants, 5,810  $\pm$  750 nm (n = 15) for the Mg4 implants, and 17.4  $\pm$  6.2 nm (n = 4) for the controls (Fig 3a).

Surface morphology analysis showed the porous surface structure of the test implants and the non-porous surface structure of the controls (Figs 3b to 3f). The mean surface porosity was 19.02%  $\pm$  0.15% (n = 3) in the Mg1 implants, 23.71%  $\pm$  0.11% (n = 3) in the Mg2 implants, 29.5%  $\pm$  1.1% (n = 3) in the Mg3 implants, and 31.52%  $\pm$  1.92% (n = 3) in the Mg4 implants. Pore size (diameter) was  $\leq$  0.5  $\mu$ m in the Mg1 implants, 1.5  $\mu$ m in the Mg2 implants, 2.5  $\mu$ m in the Mg3 implants, and 3.0  $\mu$ m in the Mg4 implants.

In regard to surface roughness, the arithmetic average height deviation (Sa) was 0.98  $\pm$  0.5  $\mu$ m for the Mg1 group, 0.78  $\pm$  0.28  $\mu$ m for the Mg2 group, 0.68  $\pm$  0.18  $\mu$ m for the Mg3 group, and 0.69  $\pm$  0.18  $\mu$ m for the Mg4 group. The developed surface ratio (Sdr), ie, the ratio of the interfacial area of a surface over the sampling area, was 46.04%  $\pm$  25.11% for the



**Fig 1** XPS survey of the surfaces of the test Mg1, Mg2, Mg3, and Mg4 implants “as received.” The spectra were recorded using normal Al K $\alpha$  radiation (1486.8 eV) with a probing beam size of 200  $\mu$ m.

Mg1 group,  $27.87\% \pm 6.99\%$  for the Mg2 group,  $26.83\% \pm 5.56\%$  for the Mg3 group, and  $32.18\% \pm 13.75\%$  for the Mg4 group. The control group had an Sa of  $0.55 \pm 0.21 \mu\text{m}$  and an Sdr of  $10.56\% \pm 3.89\%$ .

The crystal structure of x-ray diffraction (XRD) patterns indicated a mixture of anatase and rutile phases for test implants and amorphous-type crystals for controls (Fig 4). The peak intensity of rutile (110) was highest in the Mg3 implants and lowest in the Mg1 implants. The surface oxide characteristics of titanium implants used in this study are summarized in Table 1.

### Bone Responses

Figure 5 demonstrates the mean peak removal torque values (RTVs) obtained from the test and

control implants after a healing period of 6 weeks. All Mg implant groups showed significantly increased mean peak RTVs as compared to machine-turned controls ( $P \leq .05$ ). Of all implant groups, the Mg2 implant group revealed the highest RTVs. RTVs for this group were twice as high as those for machine-turned controls. Multiple comparisons of the mean peak RTVs demonstrated a highly significant difference between Mg1 implants and controls ( $P = .002$ ) and Mg2 implants and controls ( $P = .0001$ ). There were also significant differences between Mg3 and controls ( $P = .027$ ) and Mg4 implants and controls ( $P = .033$ ). When comparing the mean values between all Mg implant groups, in particular, the Mg2 implant group revealed significant differences from the Mg3

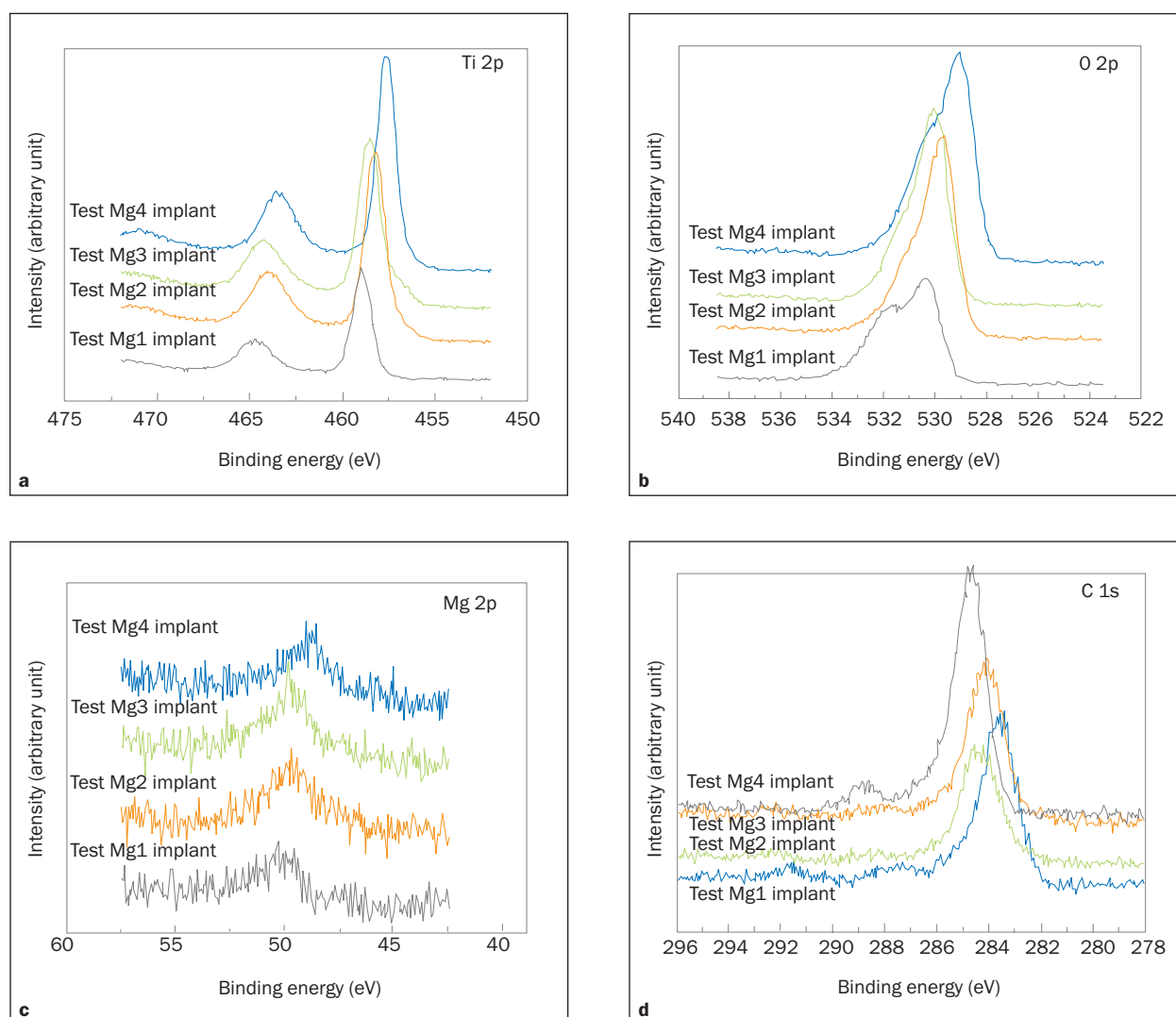


**Fig 2** XPS high resolution of the elements titanium, oxygen, magnesium, and calcium on the as-received surface.

**Table 1** Surface Oxide Characteristics of the Machine-Turned Implants (Control) and the Magnesium-Incorporated Oxidized Implants (Test)

Oxide characteristics	Implants					
	Control	Mg1	Mg2	Mg3	Mg4	
Chemical composition	Mainly TiO <sub>2</sub> with carbon contaminant	Mainly TiO <sub>2</sub> and Mg ≈ 8.36%, with carbon contaminant and traces of phosphorus and sulfur	Mainly TiO <sub>2</sub> and Mg ≈ 8.74%, with carbon contaminant and traces of phosphorus and sulfur	Mainly TiO <sub>2</sub> and Mg ≈ 8.97%, with carbon contaminant and traces of phosphorus and sulfur	Mainly TiO <sub>2</sub> and Mg ≈ 9.33%, with carbon contaminant and traces of phosphorus and sulfur	
Morphology	Nonporous	Porous	Porous	Porous	Porous	
Porosity (%)	None	19.02 ± 0.15	23.71 ± 0.11	29.5 ± 1.1	31.52 ± 1.92	
Oxide thickness nm	17 ± 6	1,060 ± 140	3,440 ± 600	5,190 ± 500	5,810 ± 750	
Crystal structure	Amorphous	Anatase + rutile	Anatase + rutile	Anatase + rutile	Anatase + rutile	
	Sa (μm)	0.55 ± 0.21	0.78 ± 0.28	0.68 ± 0.18	0.69 ± 0.18	
	Sq (μm)	0.74 ± 0.27	1.38 ± 0.8	1.1 ± 0.51	1.01 ± 0.28	
Roughness	Sds (μm <sup>2</sup> )	0.09 ± 0.03	0.09 ± 0.06	0.09 ± 0.07	0.09 ± 0.05	0.11 ± 0.04
	Sdr (%)	10.56 ± 3.89	46.04 ± 25.11	27.87 ± 6.99	26.83 ± 5.56	32.18 ± 13.75

Sa = arithmetic average height deviation; Sq = root mean square of height deviation; Sds = the number of summits in a unit sampling area; Sdr = developed surface ratio. Means ± SDs shown.

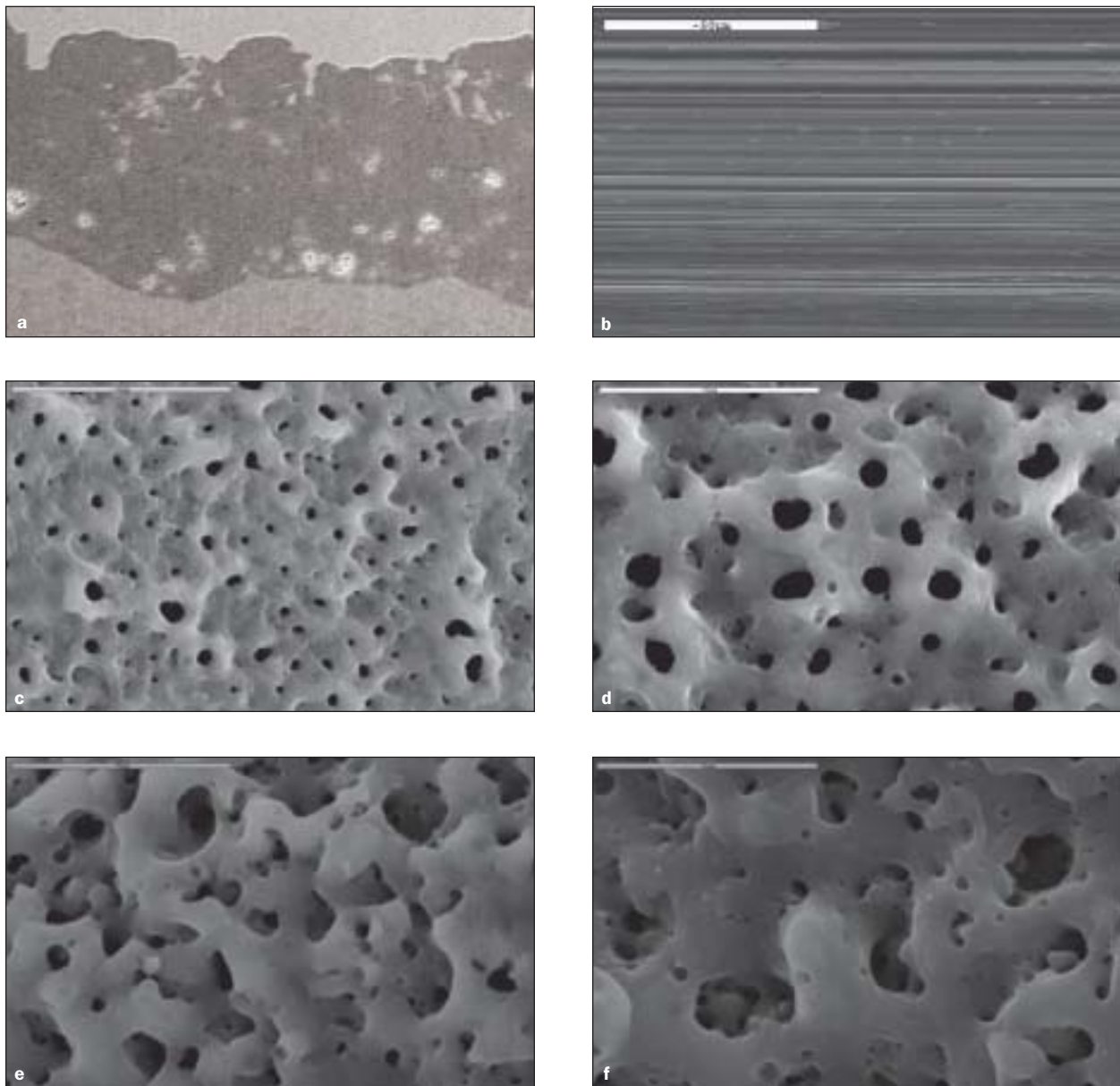


**Fig 3** Surface morphology in SEM micrographs. (a) The oxide thickness in a cross-sectional view of a test Mg2 implant. (b) A plane view of a machine-turned control implant. (c to f) Porous surface structures in (c) Mg1, (d) Mg2, (e) Mg3, and (f) Mg4 test implants.

group ( $P = .003$ ) and the Mg4 group ( $P = .027$ ), but not for the Mg1 group. However, there were no significant differences of the mean peak RTVs between Mg1, Mg3, and Mg4 ( $P > .244$ ). The mean peak RTVs were  $11.1 \pm 2.9$  Ncm (range 7 to 16 Ncm) for Mg1 implants,  $13.3 \pm 2.5$  Ncm (range 10 to 17 Ncm) for Mg2 implants,  $10.1 \pm 2.8$  Ncm (range 6 to 15 Ncm) for Mg3 implants,  $9.9 \pm 3.1$  Ncm (range 7 to 18 Ncm) for Mg4 implants, and  $6.7 \pm 1.5$  Ncm (range 4 to 9 Ncm) for machine-turned controls.

## DISCUSSION

To determine the ability of the surface properties of oxidized implants to influence bone response, the bone response was measured with the removal torque test and was analyzed as a function of quantitative changes of the surface oxide properties.

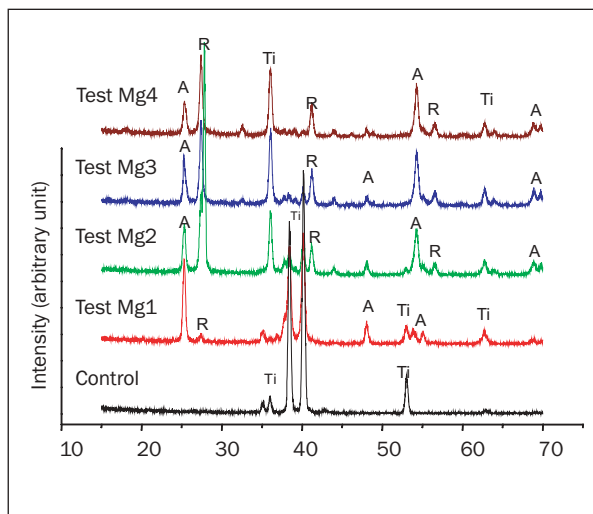


**Fig 4** XRD diffraction patterns on commercially pure titanium plates abraded by 800-grit silicon carbide (SiC) paper (controls) and oxidized in the same manner as the test implants (acceleration voltage of 35 kV and current of 25 mA). A = anatase; R = rutile; Ti = titanium.

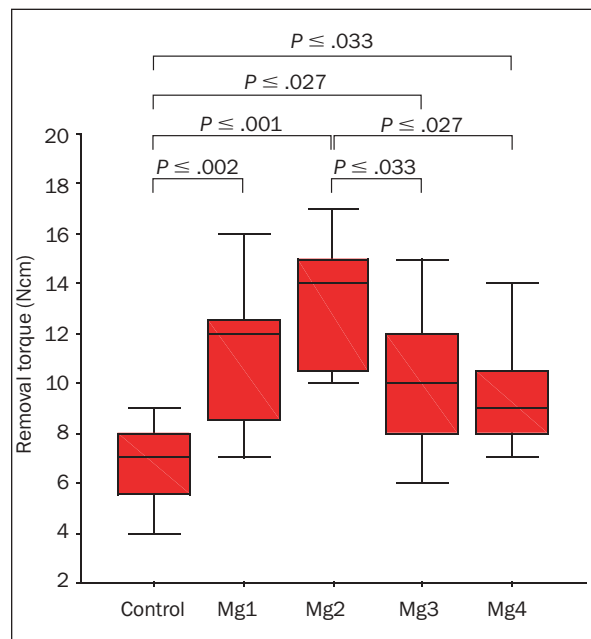


**Fig 5** Mean RTVs (Ncm) of machine-turned controls and oxidized test implants after an osseointegration period of 6 weeks.

### Magnesium Ion Concentration vs RTV

Of all the surface properties investigated in the present study, magnesium concentrations directly reflected the bone response. With increases of magnesium ion concentration in the test implants, the mean RTVs increased linearly (Fig 6). The magnesium ion concentration of  $\approx 9.3\%$  corresponded with the highest mean RTVs. Furthermore, the post hoc test performed using the Tukey method indicated that the bone response to a magnesium ion concentration of  $\approx 9.3\%$  was significantly better (ie, greater removal torque) as compared to magnesium ion concentration of  $\approx 8.3\%$  or  $\approx 8.7\%$ .

In general, the present results are in agreement with a previous report demonstrating significantly increased resonance frequency and RTVs of magnesium-incorporated oxidized test implants in a rabbit femur model (unpublished data).<sup>25</sup> The osseointegration mechanism reinforced by magnesium surface chemistry is not fully understood at present. To the best of the authors' knowledge, the importance of magnesium surface chemistry for implant integration in bone has not been demonstrated in the literature by any other laboratory. Zreiqat and colleagues<sup>26</sup> reported positive effects of  $\text{Al}_2\text{O}_3\text{-Mg}$  ceramics on cell adhesion, integrin expression, and activation of signaling proteins.

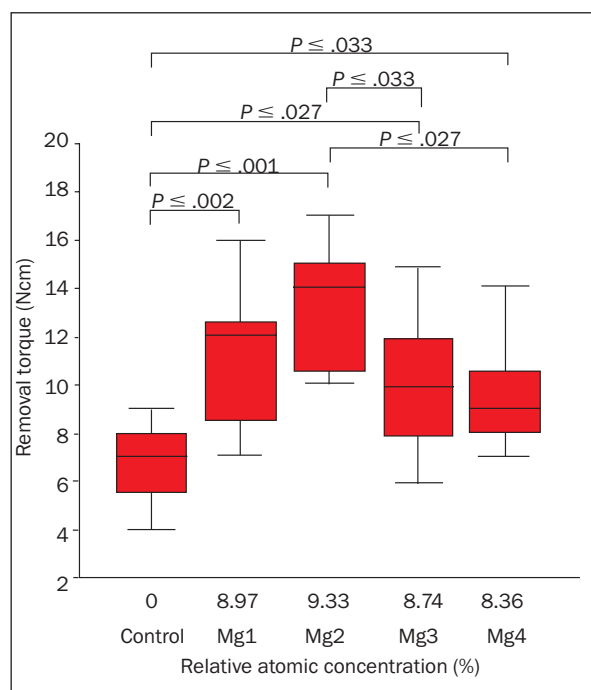


**Fig 6** Mean RTVs (Ncm) as a function of magnesium ion concentration in machine-turned controls and oxidized test implants after an osseointegration period of 6 weeks.

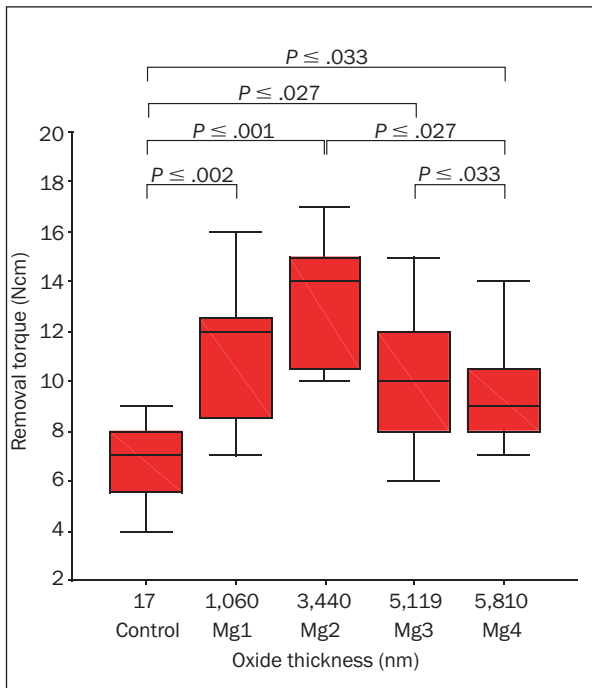


**Fig 7** Mean RTVs (Ncm) as a function of oxide thickness in machine-turned controls and oxidized test implants after an osseointegration period of 6 weeks.

### Oxide Thickness vs RTV

Mean RTVs increased as oxide thickness increased up to 3,440 nm; thereafter, they decreased as oxide thickness increased (Fig 7). The multiple comparisons post hoc test indicated that the oxide thickness of  $\approx$  3,440 nm for the Mg2 implants showed a significantly improved bone response as compared to the 5,119-nm oxide thickness of the Mg3 implants and 5,810-nm oxide thickness of the Mg4 implants ( $P = 0.033$  and  $P = .027$ , respectively). However, there was no significant difference between the mean peak RTVs of implants with an oxide thickness of 1,060 nm and those with an oxide thickness of 3,440 nm ( $P = .24$ ).

Sul and associates<sup>15-21</sup> have previously shown that in vivo bone responses to the oxidized implants are significantly improved with increases of the oxide thickness in the range of 600 to 4,000 nm as measured with resonance frequency analysis, removal torque testing, histomorphometric analysis, and enzyme histochemistry. Taken together, the present results indicate that the optimal oxide thickness for significant improvement of the bone response is likely to be about 1,000 nm for TiO<sub>2</sub>, about 1,000 to 1,200 nm for sulfur- or phosphorus-incorporated implants, and about 4,000 nm for calcium-incorporated implants. Thus, optimal oxide thickness is strongly dependent on the surface chemistry of oxidized implants and may, in fact, be dominated by it.

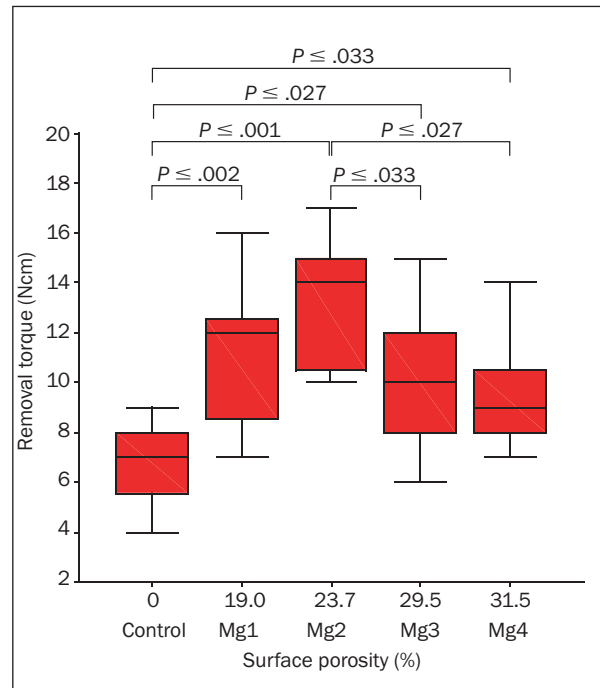


**Fig 8** Mean RTVs (Ncm) as a function of surface porosity in machine-turned controls and oxidized test implants after an osseointegration period of 6 weeks.

Kurze and coworkers<sup>27</sup> in 1986 introduced the Ti-ANOF implants (Timedur; ZL-Duraplant, Leipzig, Germany) with an average oxide thickness of 4 to 20  $\mu$ m and reported that the bone response to surface oxide properties was dependent on the anodic parameters used. Niki and colleagues<sup>28</sup> in 1992 and Ishizawa and associates<sup>29</sup> in 1995 reported strong bone response to a new implant surface anodized in a sulfuric acid and phosphoric acid (H<sub>2</sub>SO<sub>4</sub> + H<sub>3</sub>PO<sub>4</sub>) mixed electrolyte system, resulting in an oxide thickness of about 4  $\mu$ m. In 2000 Hall and Lausmaa<sup>30</sup> introduced the TiUnite implant (Nobel Biocare, Göteborg, Sweden), which was also anodized in a mixed electrolyte system containing H<sub>2</sub>SO<sub>4</sub> + H<sub>3</sub>PO<sub>4</sub>. The oxide thickness of the TiUnite implant is claimed to be 1 to 2  $\mu$ m at the coronal end, including the first threads, and 7 to 10  $\mu$ m at the apical end. Sulfur and phosphorus anions were both incorporated in the surface oxide. In 2001, Albrektsson and colleagues<sup>31</sup> reported that TiUnite oxidized implants resulted in significantly higher bone-to-metal contact values and RTVs than machine-turned implants.

### Surface Porosity vs RTV

The mean RTVs increased as porosity increased up to 23.7%; thereafter, they decreased with increased porosity (Fig 8), in the same manner as oxide thickness. This is because of the relationship



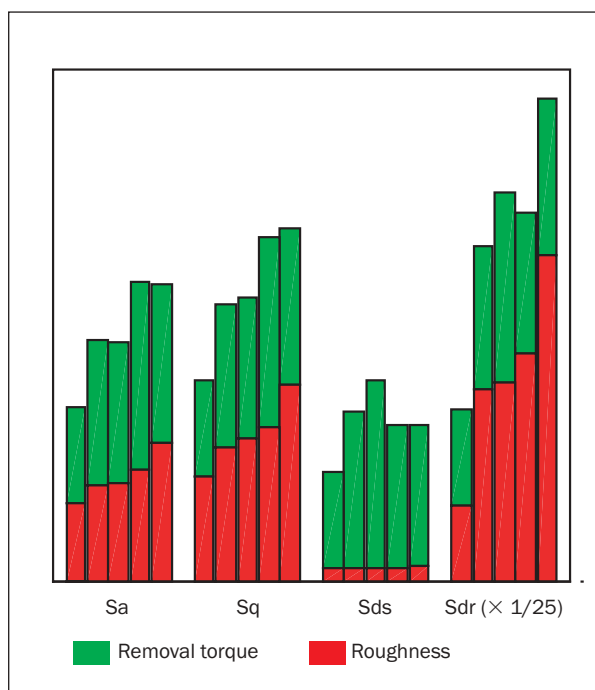


**Fig 9** Mean RTVs (%) related to changes of the roughness parameters Sa, Sq, Sds, and Sdr. This graph indicates that, of the 4 parameters, Sdr may be the most sensitive to RTV.

between oxide thickness and surface porosity. The surface porosity of opening pores increased with increased oxide thickness. Furthermore, the multiple comparisons post hoc test indicated that a surface porosity of  $\approx 23.7\%$  in the Mg2 implants showed a significantly improved bone response as compared to  $29.5\%$  in the Mg3 implants and  $31.5\%$  in the Mg4 implants ( $P = .033$  and  $P = .027$ , respectively). The mean RTVs directly increased with increased pore sizes of  $0.5 \mu\text{m}$  and  $1.5 \mu\text{m}$ ; they decreased with increased pore sizes of  $2.5 \mu\text{m}$  and  $3.0 \mu\text{m}$ . The present results support the bone response associated with pore sizes of  $0.2 \mu\text{m}$  in sulfur-incorporated implants,  $1.3 \mu\text{m}$  in phosphorus-incorporated implants, and  $1.5 \mu\text{m}$  in calcium-incorporated implants noted in previous studies.<sup>18-21</sup> The TiUnite implant is known to have a maximum pore size of 1 to  $5 \mu\text{m}$ .<sup>30</sup> Ducheyne and Qiu<sup>32</sup> reported that even with implants with test surfaces of similar porosity, the pattern and speed of bone formation were shown to be dependent on surface chemistry.

### Surface Roughness vs RTV

The mean RTVs appeared to be influenced by various roughness parameters such as Sa, Sq, Sds, and Sdr, as shown in Fig 9. Sa and Sdr may be more important roughness parameters than Sds and Sq. In addition, RTVs linearly increased with increases of Sdr up to

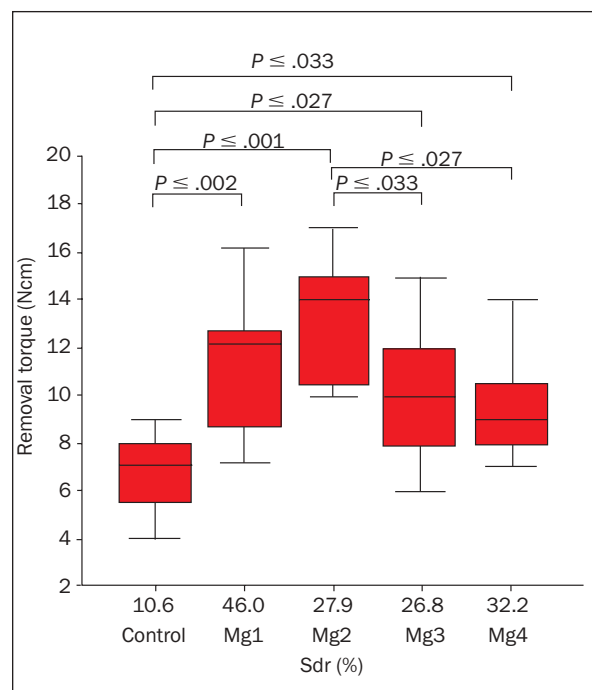


**Fig 10** Mean RTVs (%) as a function of the roughness parameter Sdr in machine-turned controls and oxidized test implants after an osseointegration period of 6 weeks.

$27.9\%$ ; thereafter they decreased as Sdr increased. Furthermore, the multiple comparisons post hoc test showed that an Sdr of about  $28\%$  in the Mg2 implant was associated with significantly improved mean RTVs as compared to an Sdr of  $32\%$  in the Mg4 implant ( $P = .027$ ) (Fig 10). With respect to Sa, an Sa of  $0.78 \mu\text{m}$  in the Mg2 implant showed the highest mean RTVs compared to means of  $0.67 \mu\text{m}$ ,  $0.69 \mu\text{m}$ , and  $0.97 \mu\text{m}$  for the other test implants and  $0.55 \mu\text{m}$  for the control. The current results demonstrated that optimal roughness values of oxidized implants were different from those reported by Wennerberg,<sup>33</sup> ie, Sa of 1 to  $1.5 \mu\text{m}$  and Sdr 1.4 to 1.5. Thus, optimal roughness values may differ from the chemical composition of the implant surface employed.

### Crystal Structure vs RTV

The mixture of anatase and rutile phases for test magnesium implants reflected significant mean RTVs as compared to amorphous phase in controls. The strongest peak intensity of the rutile phase (110) was detected in the test Mg2 implant and resulted in significantly improved bone response as compared to the mixture of anatase and rutile crystal phases seen in the test Mg3 and Mg4 implants. However, the peak intensity of rutile did not precisely correspond to the mean RTV.

The current results are congruent with previous findings that the mixture of anatase and rutile TiO<sub>2</sub> influenced bone response more than anatase structure or amorphous phase.<sup>15–17</sup> The present study showed that crystallinity was transformed with increased oxide thickness. As to the effect of crystal structure of TiO<sub>2</sub> in expression of specific phenotypes, Boyan and associates<sup>34</sup> compared chondrocyte response to TiO<sub>2</sub> of differing crystallinities and reported that cells could discriminate between surfaces at this level as well. A substantial reduction in the release of titanium ions and the role of phase transformation of crystal structure in regulating cell response may facilitate bone formation around oxidized implants and may be one reason for the results obtained in the present study.

In summary, the results of the present study clearly indicated that surface properties directly influenced the bone responses. Of all the surface properties investigated, magnesium surface chemistry in particular played a governing but not exclusive role as a determinant surface property underlying the enhanced bone response.

## CONCLUSIONS

Surface properties of implants directly influence bone responses. Thus, irrespective of the surface modification technology used, detailed surface characterization of an implant is important. Based on the bone response in the present study, which was expressed as a function of quantitative changes in the surface oxide properties, the following appear to be the “optimum” surface properties of oxidized implants:

- The optimum surface chemistry of magnesium-incorporated, oxidized implants consisted of approximately 9% magnesium at relative atomic concentration in TiO<sub>2</sub> matrix.
- The optimal oxide thickness of a porous surface structure appeared to be in the range of 1,000 to 5,000 nm.
- An optimum porosity of open pores is in the range of 19% to 30%, ie, approximately 24%; with a pore size of  $\leq 2.0 \mu\text{m}$ .
- Surface roughness values of 0.7 to 1.0  $\mu\text{m}$  for Sa, 0.9 to 1.4  $\mu\text{m}$  for Sq, and 27% to 46% for Sdr seemed to be optimum.
- TiO<sub>2</sub> in a crystalline phase, ie, a mixture of anatase and rutile phases rather than amorphous, seemed to be optimal.

## ACKNOWLEDGMENTS

This study was supported by a research grant from Biochallenge from Ministry of Science and Technology, Republic of Korea, and by MediSciTec (Korea).

## REFERENCES

1. Pham MT, Reuther H, Matz W, et al. Surface induced reactivity for titanium by ion implantation. *J Mater Sci Mater Med* 2000;11:383–391.
2. Krupa D, Baszkiewicz J, Kozubowski JA, et al. Effect of calcium-ion implantation on the corrosion resistance and biocompatibility of titanium. *Biomaterials* 2001;22:2139–2151.
3. Bosetti M, Masse A, Tobin E, Cannas M. In vivo evaluation of bone tissue behavior on ion implanted surfaces. *J Mater Sci Mater Med* 2001;12:431–435.
4. De Maezta MA, Alava JI, Gay-Escoda C. Ion implantation: Surface treatment for improving the bone integration of titanium and Ti6Al4V dental implants. *Clin Oral Implants Res* 2003;14: 57–62.
5. Kimura H, Horng CJ, Okazaki M, Takahashi J. Oxidation effects on porcelain-titanium interface reactions and bond strength. *Dent Mater J* 1990;9:91–99.
6. Taira Y, Matsumura H, Yoshida K, Tanaka T, Atsuta M. Influence of surface oxidation of titanium on adhesion. *J Dent* 1998;26:69–73.
7. Ducheyne P. Effect of bioactive glass particle size on osseous regeneration. *J Biomed Mater Res* 1999;46:301–304.
8. Oonishi H, Hench LL, Wilson J, et al. Quantitative comparison of bone growth behavior in granules of Bioglass, A-W glass-ceramic, and hydroxyapatite. *J Biomed Mater Res* 2000;51: 37–46.
9. Nishiguchi S, Kato H, Fujita H, et al. Titanium metals form direct bonding to bone after alkali and heat treatments. *Biomaterials* 2001;22:2525–2533.
10. Ivanoff CJ, Widmark G, Johansson C, Wennerberg A. Histologic evaluation of bone response to oxidized and turned titanium micro-implants in human jawbone. *Int J Oral Maxillofac Implants* 2003;18:341–348.
11. Rocci A, Martignoni M, Gottlow J. Immediate loading of Brånemark System TiUnite and machined-surface implants in the posterior mandible: A randomized open-ended clinical trial. *Clin Implant Dent Relat Res* 2003;5(suppl 1):57–63.
12. van Steenberghe D. Address from the Basic Science Committee. In: van Steenberghe D (ed). *Tissue Integration in Oral and Maxillo-Facial Reconstruction: Proceedings of an International Congress*. New York: Excerpt Medica, 1986.
13. Sul YT, Johansson CB, Jeong Y, Albrektsson T. The electrochemical oxide growth behaviour on titanium in acid and alkaline electrolytes. *Med Eng Phys* 2001;23:329–346.
14. Sul YT, Johansson CB, Petronis S, et al. Characteristics of the surface oxides on turned and electrochemically oxidized pure titanium implants up to dielectric breakdown: The oxide thickness, micropore configurations, surface roughness, crystal structure and chemical composition. *Biomaterials* 2002;23:491–501.
15. Sul YT, Johansson CB, Jeong Y, Wennerberg A, Albrektsson T. Resonance frequency and removal torque analysis of implants with turned and anodized surface oxides. *Clin Oral Implants Res* 2002;13:252–259.
16. Sul YT, Johansson CB, Jeong Y, Roser K, Wennerberg A, Albrektsson T. Oxidized implants and their influence on the bone response. *J Mater Sci Mater Med* 2001;12:1025–1031.
17. Sul YT, Johansson CB, Roser K, Albrektsson T. Qualitative and quantitative observations of bone tissue reactions to anodized implants. *Biomaterials* 2002;23:1809–1817.

18. Sul YT, Johansson CB, Kang Y, Jeon DG, Albrektsson T. Bone reactions to oxidized titanium implants with electrochemical anion sulphuric acid and phosphoric acid incorporation. *Clin Implant Dent Relat Res* 2002;4:78–87.
19. Sul YT, Johansson CB, Albrektsson T. Oxidized titanium screws coated with calcium ions and their performance in rabbit bone. *Int J Oral Maxillofac Implants* 2002;17:625–634.
20. Sul YT. The significance of the surface properties of oxidized titanium to the bone response: Special emphasis on potential biochemical bonding of oxidized titanium implant. *Biomaterials* 2003;24:3893–3907.
21. Sul YT, Byon ES, Jeong Y. Biomechanical measurements of calcium-incorporated oxidized implants in rabbit bone: Effect of calcium surface chemistry of a novel implant. *Clin Implant Dent Relat Res* 2004;6:101–110.
22. Sul YT. On the Bone Response to Oxidized Titanium Implants: The Role of Microporous Structure and Chemical Composition of the Surface Oxide in Enhanced Osseointegration [thesis]. Göteborg, Sweden: Göteborg Univ, 2002.
23. Jerrold HZ. *Biostatistical Analysis*. London: Prentice-Hall, 1984:186–222.
24. Johansson CB. On Tissue Reactions to Metal Implants [thesis]. Göteborg, Sweden: Göteborg Univ, 1991.
25. Sul YT, Johansson P, Chang BS, Byon ES, Jeong Y. Bone tissue responses to Mg-incorporated oxidized implants and machine-turned implants in the rabbit femur. *J Appl Biomater Biomechanics* (in press).
26. Zreiqat H, Howlett CR, Zannettino A, et al. Mechanisms of magnesium-stimulated adhesion of osteoblastic cells to commonly used orthopaedic implants. *J Biomed Mater Res* 2002; 62:175–184.
27. Kurze P, Krysmann W, Knofler W. ANOF – ein neues Beschichtungsverfahren für die medizintechnik. *Stomatologie der DDR* 1986;36:549–554.
28. Niki M, Ito G, Matsuda T, Orgino M. Comparative push-out data of bioactive and non-bioactive materials of similar rugosity. In: Davies JE (ed). *The Bone-Biomaterials Interface*. Toronto, Canada: University of Toronto Press, 1991:350–356.
29. Ishizawa H, Fujino M, Ogino M. Histomorphometric evaluation of the thin hydroxyapatite layer formed through anodization followed by hydrothermal treatment. *J Biomed Mater Res* 1997;35:199–206.
30. Hall J, Lausmaa J. Properties of a new porous oxide surface on titanium implants. *Appl Osseointegration Res* 2001;1:5–8.
31. Albrektsson T, Johansson C, Lundgren AK, Sul YT, Gottlow J. Experimental studies on oxidized implants. A histomorphometrical and biomechanical analysis. *Appl Osseointegration Res* 2000;1:21–24.
32. Ducheyne P, Qiu Q. Bioactive ceramics: The effect of surface reactivity on bone formation and bone cell function. *Biomaterials* 1999;20:2287–2303.
33. Wennerberg A. On Surface Roughness and Implant Incorporation [thesis]. Göteborg, Sweden: Göteborg Univ, 1996.
34. Boyan BD, Hummert TW, Dean DD, Schwartz Z. Role of material surfaces in regulating bone and cartilage cell response. *Biomaterials* 1996;17:137–146.